Transient Stability Improvement by Pre-fault and Post-fault modifications in Wind Power Plant Control

Niloy Patari
Department of Electrical Engineering
Indian Institute of Technology
Kharagpur, India
niloyee30@gmail.com

Dheeman Chatterjee
Department of Electrical Engineering
Indian institute of Technology
Kharagpur, India
dheemanc@gmail.com

Tanmoy Bhattacharya
Department of Electrical Engineering
Indian Institute of Technology
Kharagpur, India
btanmoy@ee.iitkgp.ernet.in

***Abstract*—This paper proposes some modifications in the interfacing power converter control of a permanent magnet synchronous generator (PMSG) based Wind Power Plant with the aim of improving transient stability of the power system. Since the wind speed varies over time and the converters are designed for the rated capacity, they remain unutilized during low wind speed condition. This paper proposes a modified operation during pre-fault and post-fault steady state conditions where the balanced capacity is utilized to maintain the terminal voltage of the wind power plant. In a further proposed modification, the wind power plant terminal frequency deviation is used to modulate its terminal voltage. This is applied only for a small duration (about 1 second) just after the fault clearance. The effectiveness of both the proposed modified operation is investigated in the WSCC 3-machine 9-bus system using PSCAD/EMTDC platform. The study was carried out considering fault at different locations in the system and with various wind speed conditions.**

Keywords-*Transient stability, wind energy, permanent magnet synchronous generator.*

I. INTRODUCTION

With fossil fuels being on the verge of depletion, renewable energy integration like wind and solar energy is the only alternative left to meet increasing power demands globally. Variable speed wind turbine driven generators like doubly fed induction generators (DFIGs), permanent magnet synchronous generators (PMSGs) are quite popular nowadays. PMSG is the newest prospect among all wind generators since it provides high power density and absence of slip rings, gearboxes and excitation coils makes the generation system maintenance free and efficient. Moreover, the power electronic interfacing converters can be controlled easily to extract maximum power from wind turbines and subsequently control active and reactive power injection to the grid [1].

Wind energy being variable in nature, the generation systems also inject variable power to the grid and hence affect power system dynamics considerably. In addition to this, presence of interfacing converters reduces the system inertia and also affects the synchronizing power and damping power of the system [2]. Impacts of wind energy on power systems are studied in [3-8]. In recent times, lot of research is going on active participation of wind farms in power systems as in [9]. One such example is presented in [10] where the interfacing power converters of the DFIG based wind farm are controlled in the post-fault duration to improve transient stability of power systems. However, no such research work has been done on enhancing transient stability of power systems in presence of PMSG based wind power plants. This paper presents two control modifications and an additional post-fault modification in the interfacing converter control strategies to enhance transient stability. The control modifications are explained below.

Under normal conditions, the wind power plant generates less power than its rated power capacity since the wind experienced by the turbine blades is variable in nature and seldom reaches its rated value. PMSG based wind power plants being integrated to the grid by back to back voltage sourced converters; the grid side converter (GSC) sends less active power than its rated capacity. In the first method, the GSC is controlled to inject the balance inverter current (maximum inverter current reduced by the active component of inverter current) as reactive current to the grid at steady state. In the second method, the GSC is controlled to maintain the power plant terminal voltage at a nominal value of 1 pu. Both these control modifications are investigated and compared through simulations in WSCC 3-machine 9-bus system. However, the second method works well in all possible conditions and enhances transient stability unlike the first method. Another modification in the post-fault period is also proposed where the terminal frequency deviation is used to modulate the power plant terminal voltage for a small period. However, this is operative for a small duration (1 second after fault clearance) and after this small post-fault duration, the converter controls resemble that of the proposed second method (i.e. the wind power plant is controlled to maintain its terminal voltage to a nominal value). The second method along with this post-fault modification is simulated in PSCAD/EMTDC and is validated to improve transient stability in WSCC 3-machine 9-bus system.

II. NORMAL OPERATION OF PMSG BASED WIND POWER PLANT

A. Modelling of PMSG based Wind Power Generation System

A variable speed wind turbine driven permanent magnet synchronous generator (PMSG) is integrated to the grid through a fully rated back to back voltage source converter (VSC) followed by a coupling transformer as shown in Fig. 1. The machine side converter (MSC) is controlled to extract maximum power from the wind turbine and dump it to the interconnecting dc link. The grid side converter (GSC) helps in evacuating this power to the gird and enables decoupled control of active and reactive power injection by the power plant. An aggregated wind turbine and generator model is considered here since the work involves studying impacts of PMSG based wind power plants on transient stability aspects of the power system [11].

A single mass turbine generator shaft model is considered. The electro-mechanical dynamics of the coupled rotor is represented as in [12]

$$\frac{d\omega_r}{dt} = \frac{1}{J}\left(T_m - T_e - B\omega_r\right) \quad (1)$$

Where ω_r represents the angular velocity of the rotor, T_m and T_e are the mechanical and electromagnetic torque respectively. J is the combined inertia constant of turbine and generator rotor and B is viscous friction coefficient.

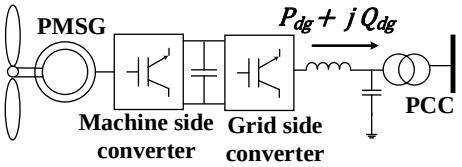

Fig. 1. PMSG-based Wind Power Generation system

B. Control of the Machine Side Converter

Maximum power point tracking in the MSC is accomplished by setting the electromagnetic torque as in (2). However, for rotor speeds greater than the rated rotor speed, the electromagnetic torque reference is set to its rated value(T_{rated}) to avoid overloading of the converters downstream. This is the pitch angle control of the wind power plant.

$$T_{ref} = K_{opt}\omega_r^{\,2} \text{ if } \omega_r < \omega_{rated}, V_g > 0.9\,pu \quad (2)$$
$$= T_{rated} \text{ if } \omega_r > \omega_{rated}, V_g > 0.9\,pu$$

$$K_{opt} = \frac{1}{2}\rho\pi R^5 C_{p\max}\omega_r^2 / \lambda_{opt}^3 \quad (3)$$

Whereλ_{opt} is the optimal tip-speed ratio, R is the turbine radius, C_{pmax} is the maximum value of power coefficient, V_g is the grid voltage.

An interior type PMSM (IPMSM) suitable for high power applications has been considered in this work. Maximum torque per ampere (MTPA) control is implemented in the MSC control strategy in order to exploit the reluctance torque of IPMSM fully [13]. The optimized *d*-axis and *q*-axis MSC reference currents $\left(I_{dmref}, I_{qmref}\right)$ are calculated depending on the given torque reference (4-5) [14]. I_{dmref}, I_{qmref} are input to the inner current control loops and generate the reference *d*-axis and *q*-axis stator voltages $\left(V_{dmref}, V_{qmref}\right)$. The control structure is shown in Fig. 2. L_d and L_q are the *d*-axis and *q*-axis stator inductances and Ψ_f is the rotor flux. Three phase stator voltage references are generated from (V_{dmref}, V_{qmref}) by *d*-*q*-o to *a*-*b*-*c* transformation, which are then used in the pulse width modulation to get the converter switching pulses.

$$\frac{I_{dmref}}{I_b} = 0.01\frac{T_{ref}^2}{T_b^2} - 0.298\frac{T_{ref}}{T_b} + 0.0481 \quad (4)$$

$$\frac{I_{qmref}}{I_b} = \frac{-2}{3\left(1 - \frac{I_{dref}}{I_b}\right)}\frac{T_{ref}}{T_b} \quad (5)$$

Here $T_b = \Psi_f p_f I_b$, $I_b = \frac{\Psi_f}{(L_q - L_d)}$, L_d and L_q are the *d*-axis and *q*-axis stator inductances, p_f is the number of pole pairs and Ψ_f is the rotor flux.

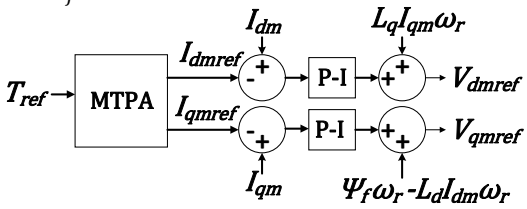

Fig. 2. MTPA Implementation in MSC Control

C. Control of the Grid Side Converter

The *d*-axis of the synchronously rotating reference frame is oriented along the grid voltage (V_g) thus enabling decoupled control of active and reactive power by the GSC. The active power injection to the grid $\left(P_{dg}\right)$ is now solely dependent on the *d*-axis component of the inverter current (I_{gd}) whereas the *q*-axis inverter current $\left(I_{gq}\right)$ determines the reactive power injection $\left(Q_{dg}\right)$ by the power plant as shown in (6-7) [15].

$$P_{dg} = \frac{3}{2}V_g i_{gd} \quad (6)$$

$$Q_{dg} = -\frac{3}{2}V_g i_{gq} \quad (7)$$

The dc-link capacitor voltage dynamics is shown below-

$$C\frac{dV_{dc}}{dt} = \frac{1}{V_{dc}}\left(P_m - P_{dg}\right) \quad (8)$$

Where C represents the dc-link capacitor and P_m is the active power injection by the MSC to the dc-link.

Grid side converter (GSC) control strategy consists of a slower outer dc link voltage control and inner fast current control loops. The outer voltage control loop maintains the dc-link capacitor voltage (V_{dc}) at a certain reference voltage (V_{dcref}) and thereby enables passage of active power from MSC to the grid. The complete control structure of GSC is shown in Fig. 3 [15]. The outer dc-link voltage controller generates the reference *d*-axis grid current (I_{gdref}) which is then input to the inner *d*-axis current control to generate the reference *d*-axis inverter terminal voltage (V_{gdref}). Reactive power exchange can be controlled by setting the reference *q*-axis current

(I_{gqref})accordingly as in (7). Under normal (steady state) condition, I_{gqref} is set to zero for unity power factor operation of the power plant. I_{gqref} is then input to the inner *q*-axis current control loop to generate the reference *q*-axis inverter terminal voltage (V_{gqref}).V_{gdref} and V_{gqref} are then transformed to the corresponding *a-b-c* reference voltages using *d-q*-o to *a-b-c* transformation.

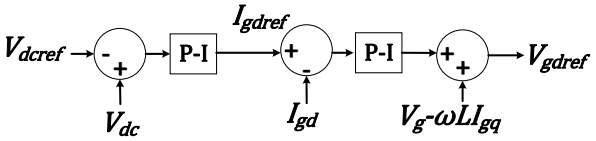

Fig. 3(a). *d*-axis control of GSC

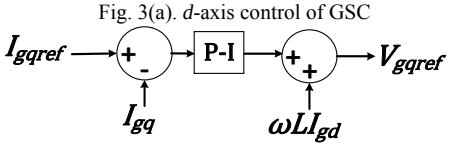

Fig. 3(b). *q*- axis control of GSC

D. Low Voltage Ride Through (LVRT) capability of the Wind Power Plant

However, when wind power plant terminal voltage (V_g) falls below a certain limit, the active power injection by the GSC gets limited too since the GSC current hits the converter current limits. As a result, the power extracted by the MSC cannot be fully evacuated by the GSC. The result is an increase in the dc link voltage. To avoid this dc-link capacitor overvoltage, the PMSG electromagnetic torque reference is modulated as shown in Fig. 4. The MSC control strategy now includes a dc-link voltage controller which sets the reference electromagnetic torque to a reduced value (T_{lvrt}) and thus the dc-link overvoltage is mitigated. The power plant, however, still remains connected to the grid and sends a reduced value of active power to the grid. Here V_{dcref} and P_t represent reference dc-link voltage and the GSC terminal active power injection respectively. This is the low voltage ride through (LVRT) strategy of the wind power plant [16]. The voltage limit, below which LVRT is activated, is set at 0.9 pu in this work.

This operation of wind power plant as described in this section can be denoted as Normal Mode of operation.

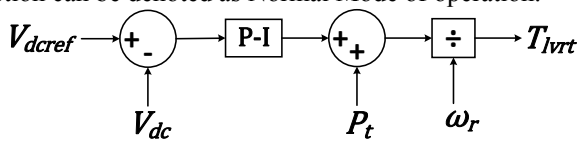

Fig. 4.Control of PMSG during LVRT

III. Proposed Modifications in Wind Power Plant Control to Enhance Transient Stability

During a three phase short-circuit fault, the electromagnetic power output of alternators (P_e) reduce considerably owing to sudden dip in their terminal bus voltages. The mechanical power input to the alternators (P_m), however, remains unchanged during the short fault duration. The resultant difference in the mechanical and electrical power output of alternators ($P_m - P_e$) being high during fault, the rotors of the alternators accelerate. This excursion of the rotor angle if not restricted may lead to angular instability of the system. If, however, the pre-fault alternator terminal voltages are high enough, pre-fault rotor angles will be low to serve the same power system loads. Transient stability margin is thus increased. Two modified control strategies (*Case*1 and *Case* 2) of the wind power plant are hence proposed in this context. The primary motive of these methods would be to keep the pre-fault alternator terminal voltages at a higher value and hence a lower pre-fault rotor angle.

Case 1 Wind turbines experience variable wind speeds throughout the year and for wind speeds less than the rated wind speed, the power outputs of the power plants are also less than their rated capacities. Hence, unless the wind blows at its rated speed, the grid side converter (GSC) current never reaches its rated value and there is always a balance current (the maximum inverter current reduced by the active component of inverter current) left unutilized by the GSC. This method proposes the balance inverter current to be injected as reactive current to the grid at steady state. Reactive power being injected, the power plant terminal voltage is boosted. Terminal voltages of the alternators placed near the wind power plant are boosted too. The pre-fault rotor angle of alternators is thus reduced to serve the same power system load. The result is an improvement in the transient stability margin of power systems.

The modified control strategy is shown in Fig. 5. The MSC controls as in Fig. 2 remains unchanged in this mode of operation. However, the GSC *q*-axis current control is modified as in Fig. 5 but the *d*-axis current control remains the same as in Fig. 3.

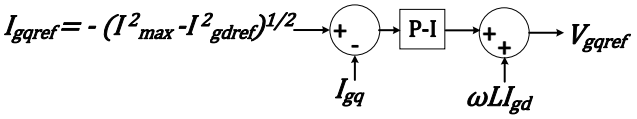

Fig. 5. Modified *q*- axis control of GSC under *Case* 1 operation

Case 2 In this method, the balance current of the GSC is utilized to maintain the power plant terminal voltage to a nominal value at steady state. This, however, boosts the terminal voltages of the alternators placed near the wind power plant. Hence, the alternator pre-fault rotor angle is also low and hence improves the transient stability of power systems.

The modified control strategy for *Case* 2 operation is shown in Fig. 6. The MSC controls remain unchanged as shown in Fig. 2. The *d*-axis current control also remains same as in Fig. 3. However, the GSC *q*-axis current control is modified to maintain the power plant terminal voltage at its nominal value ($V_{ref} = 1\,pu$) as in Fig. 6. The outer terminal voltage controller consists of a P-I controller which provides the necessary *q*-axis current command to the inner current loop. The *q*-axis current command generated is, however, limited by the maximum balance current limits (I_{gqmax}, I_{gqmin}) as in (9, 10).

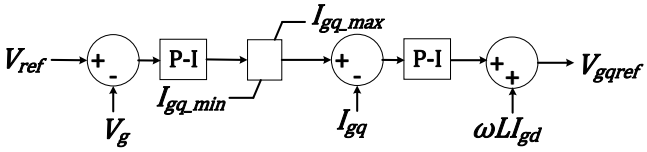

Fig. 6. Modified *q*- axis control of GSC under *Case* 2 operation

$$I_{gq\,max} = \sqrt{I_{max}^2 - I_{gdref}^2} \tag{9}$$

$$I_{gq\,min} = -\sqrt{I_{max}^2 - I_{gdref}^2} \qquad (10)$$

However, there is a notable difference between the operational principle of *Case* 1 and *Case* 2 modifications. In *Case* 1, both in pre-fault and after fault clearance, the reactive current reference (I_{gqref}) is always in negative sense which means that reactive power is always being injected by the GSC to the grid. However, in *Case* 2, the reactive current reference (I_{gqref}) is generated to maintain the power plant terminal voltage at ($V_{ref} = 1\,pu$). Hence, at steady state and after fault clearance, GSC may inject or absorb reactive power from the grid to maintain its terminal voltage at 1 pu.

IV. Application of the Proposed Modifications in WSCC 3-Machine 9-Bus System

Next, the WSCC 3-machine 9-bus system (shown in Fig. 7) is considered to validate the effectiveness of the proposed methods. A PMSG based wind power plant of rating 100 MW is connected at bus 8. The total load connected in the 9-bus system is 315 MW [17]. Since the proposed modified operations involve modifications in converter control, the PSCAD/EMTDC simulation platform is used. It includes the detailed dynamics of the converters, PMSG and the synchronous generators. An additional local load ($P_l + jQ_l$) is also considered to be connected at bus 8. Thus, under steady state the average power from the wind power plant matches the additional load and the steady state power flow in the 9-bus system remains unchanged as had been the case with no wind power plant[18].However, under system disturbances, the wind farm interacts with the 9-bus system and influences its stability.

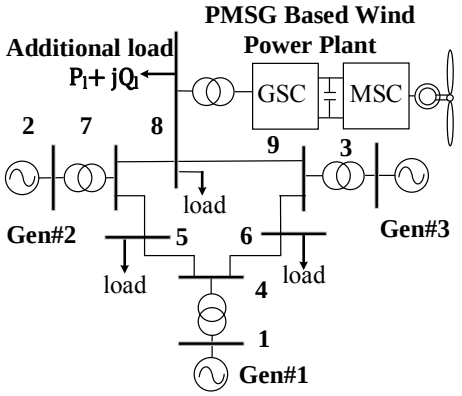

Fig.7. WSCC 3-machine 9-bus system with wind farm connected at bus 8.

A. Modelling of Power System Network and Synchronous Machines

Flux decay model is used to represent synchronous machines [17,19]. A simplified exciter with one gain and one time constant is considered here [19]. The transmission lines are represented by nominal-π model. The generator and exciter dynamical equations are given as follows.

$$\frac{d\delta_i}{dt} = \omega_s \Delta\omega_{r_i} \qquad ,i = 1,.....m \qquad (11)$$

$$2H_i \frac{d\Delta\omega_{r_i}}{dt} = P_{m_i} - P_{e_i} - K_{D_i}\Delta\omega_{r_i} \quad ,i = 1,.....m \qquad (12)$$

$$T_{do_i}\frac{dE'_{q_i}}{dt} = \frac{-x_{d_i}}{x'_{d_i}}E'_{q_i} + \left(\frac{x_{d_i}}{x'_{d_i}} - 1\right)V_i\cos(\delta_i - \theta_i) + E_{fd_i}$$
$$,i = 1,.....m \qquad (13)$$

$$T_{A_i}\frac{dE_{fd_i}}{dt} = -E_{fd_i} + (V_{ref_i} - V_i)K_{A_i} \quad ,i = 1,.....m \qquad (14)$$

$$P_{e_i} = E'_{q_i}V_i\sin(\delta_i - \theta_i)/x'_{d_i}$$
$$+0.5\left(\frac{1}{x_q} - \frac{1}{x'_d}\right)V_i^2\sin 2\left(\delta_i - \theta_i\right) \quad ,i = 1,.....m \qquad (15)$$

Where H is the inertia constant, Δw_{ri} is speed deviation of the synchronous generator rotor, P_m is the steam input, P_e is the electrical power output, K_D is the damping coefficient, δ is the rotor angular position, T'_{do} is the d-axis open circuit time constant,x'_d is d-axis transient reactance, E'_q is q-axis voltage behind x'_d , x_d and x_q are d-axis and q-axis synchronous reactance respectively,V is the terminal voltage of the alternator, θ is the terminal voltage angle, K_A and T_A are exciter gain and time constant respectively andE_{fd} is the exciter voltage.

B. Study with variable wind speed

A typical profile of the wind speed variation over 100s is considered with wind speeds varying between 9m/s and 15m/s as shown in Fig. 8[10]. The power generation by the power plant thus varies between 42% and 100% (the rated wind speed is 12m/s).Three distinct instants 'X'(t=26.5s), 'Y'(t=33s), and 'Z'(t=36s) are considered as fault instants as shown in Fig. 8.

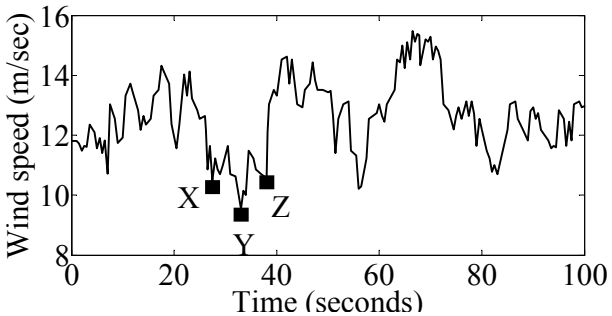

Fig. 8. Variable wind profile

C. Simulation Results

Three phase self-clearing faults are created at bus 4 and bus 5 at the fault instants 'X', 'Y', 'Z' one at a time. The proposed modifications (*Case* 1 and *Case* 2) in the control strategy of the wind power plant are simulated in PSCAD/EMTDC platform. These methods are, however, operative in the pre-fault conditions and after fault clearance only. Critical clearing time (CCTs) for both proposed methods and normal operation of the wind power plant (Sec II) for short circuit faults at bus 4 and bus 5 at the given fault instants are calculated and are shown in Table I. CCT is defined as the time within which if the short-circuit fault is not cleared, the system becomes unstable. CCT, hence, is one of the important parameters that quantifies transient stability of power systems.

TABLE I
Comparison of CCT for Normal, *Case*1 and *Case* 2 Operation

Fault Location	Fault Instants	CCT (ms)				
		Normal	*Case*1	Change	*Case* 2	Change
Bus 4	X	251	380	**129**	254	**3**
	Y	303	378	**75**	324	**21**
	Z	352	355	**3**	360	**8**
Bus 5	X	331	486	**155**	333	**2**
	Y	424	375	**-49**	492	**68**
	Z	521	470	**-51**	576	**55**

From the table, it is clear that *Case* 1 modification deteriorates transient stability of power systems when compared to normal mode of operation at certain fault instants. For example, CCTs obtained for Normal mode of operation for three phase faults at bus 5 at instants 'Y' and 'Z' are 424 ms and 521 ms respectively. The CCTs obtained for the above cases for Case 1 modification are 375 and 470 ms respectively. However, the CCTs obtained for *Case* 2 modification for these particular cases are 492 ms and 576 ms respectively and hence an improvement of 68 ms and 55 ms respectively. *Case* 2 modification also improves CCT values for all fault instants considered as shown in the table. Hence, it confirms *Case* 2 as a better choice among *Case* 1 and *Case* 2 modifications towards improving transient stability.

The reason behind the effectiveness of *Case* 2 modification towards transient stability improvement can be explained by the fact that in this method, the power plant control strategy is modulated to maintain its terminal voltage at 1 pu. Hence, after fault clearance when the power system is subjected to post-fault oscillations, bus voltage swings are somehow restricted in the range of 1 pu. On the other hand, no such control strategy is implemented in *Case* 1 modification. Instead, the power plant injects reactive power to the grid which leads to subsequent increase in its terminal bus voltage in the post-fault duration. Hence, there is no restriction on bus voltage swings in the post-fault period.

(i) *Effect of Case* 2 *operation*:

Let us consider a self-clearing short circuit fault of duration 425 ms at bus 5 at fault instant 'Y'(t=33s). Hence the fault is created at t=33s and cleared at t=33.425s. However, a delay of 50 ms is considered which accounts for the detection and activation of control signals implemented in the control strategies of the GSC and MSC. This means the MSC and GSC controls are activated 50 ms after the instant of fault inception at (t=33+0.05=33.05s) and fault clearance at (t=33.425+0.05=33.475s).

The variation of wind power plant terminal voltage at bus 8 (V_8) is shown in Fig. 9. For normal mode of operation, the GSC q-axis reference current is always set to zero. However, under *Case* 2 mode of operation, the q-axis current control is modified to maintain the power plant terminal voltage at ($V_{ref} = 1pu$) at steady state (during pre-fault and after fault clearance) as in Sec. III. This is clear from Fig. 9. Though, the pre-fault power plant terminal voltages (V_8) for both modes of operation are almost equal, after fault clearance, the power plant under *Case* 2 makes an effort to maintain its terminal voltage at 1 pu.

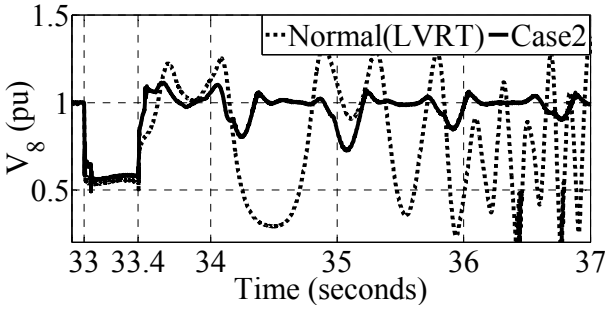

Fig. 9. Variation of wind power plant terminal voltage (V_8) under (i) Normal and (ii) *Case* 2 operation

Since V_8 is higher for *Case* 2 operation than that of the normal mode after fault clearance, it affects the nearby alternators too. The terminal voltage of the alternator 2 (V_2) at bus 2 gets boosted as shown in Fig. 10.

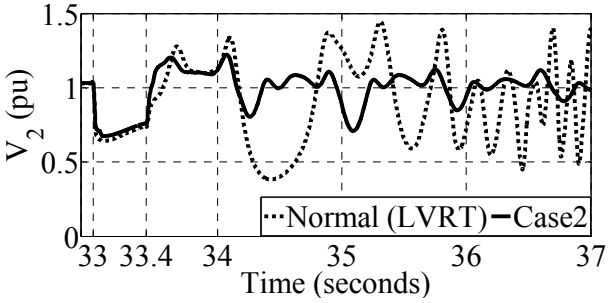

Fig. 10. Variation of alternator 2 terminal voltage (V_2) under (i) Normal and (ii) *Case* 2 operation

This results in an increased alternator power output (P_2) for *Case* 2 mode of operation as shown in Fig. 11. Alternator power being increased, this decreases the imbalance between the mechanical power of alternator 2 and its electric power output and restricts further excursion of the alternator rotor angle (δ_{21}), thus enhancing transient stability. The rotor angle (δ_{21}) is bounded for *Case* 2 operation whereas it becomes unbounded for normal mode of operation as shown in Fig. 12.

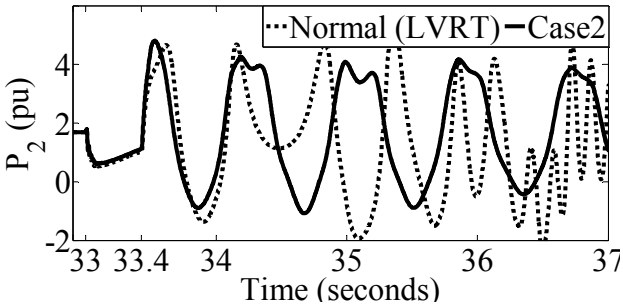

Fig. 11. Variation of alternator 2 output power (P_2) under (i) Normal and (ii) *Case* 2 operation

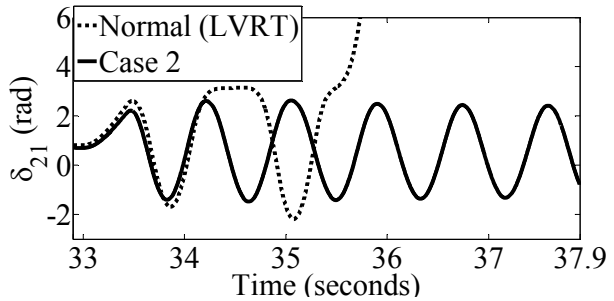

Fig. 12. Variation of relative rotor angle (δ_{21}) under (i) Normal and (ii) *Case* 2 operation

V. Proposed Postfault Modification and its Application in WSCC 3-Machine 9-Bus System

A. Postfault Modification(PFM)

An additional modification in power plant control strategy is introduced in this work [20]. This method modifies the power plant terminal voltages taking the power plant terminal frequency deviation ($\Delta f = f^*_{WPP} - f_{WPP}$) into consideration as in Fig. 13. The frequency deviation is input to a low pass filter (LPF) which extracts the low frequency component of Δf(1-2 Hz). The output is then passed to a phase compensator (lead-lag compensator) which compensates the phase lag introduced by the low pass filter while extracting the low frequency component of Δf. The phase compensator output is now input to a PI compensator which provides the required deviation in the power plant terminal voltage (ΔV_{ref}). ΔV_{ref} when passed through a PI compensator generates a *q*-axis GSC current command (ΔI_{gqref}). ΔI_{gqref} is added with the reference current command ($I_{gqref} = 0$) to generate the modified reference *q*-axis GSC current command (I^*_{gqref}). I^*_{gqref} is then input to the usual current control loop as shown in Fig. 3(b). The modified *q*-axis current reference (I^*_{gqref}) thus modulates the power plant terminal voltage taking the deviation of frequency into account. Terminal voltage of alternator placed near the power plant gets modulated too as a result. This in turn affects the alternator power outputs and hence transient stability of power systems. It is to be noted that the PI compensator following the phase compensator must be designed suitably in order to achieve substantial improvement in the transient stability margin.

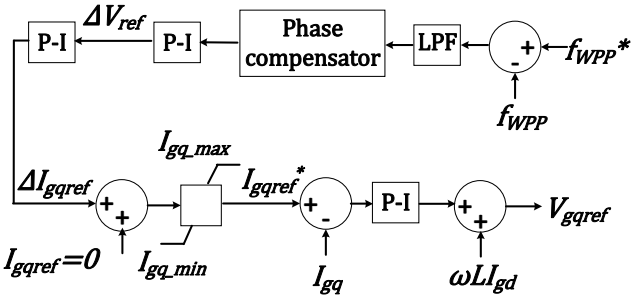

Fig. 13. Post-fault modification

B. Effect of Postfault Modification(PFM)

Self-clearing three phase faults are simulated at bus 4 and bus 5 at fault instants 'X', 'Y' and 'Z' as shown in Fig. 8. The CCT obtained for *Case* 2 mode of operation at 'Y'(t=33s) at bus 5 is found to be 492 ms as shown in Table I. Now, a self-clearing fault of 493 ms is simulated at bus 5 at fault instant 'Y'. A time delay of 50 ms is considered here to account the detection and activation of control signals in MSC and GSC control structures. *Case* 2 and *Case* 2 with PFM modes of operation are simulated in PSCAD/EMTDC platform and are now compared in the following figures.

The three phase fault is cleared at t=33+0.493s (t=33.493s). However, the control algorithms start their action 50ms after fault clearance i.e. at t=33.493+0.05s (t=33.543s). Thus, for *Case* 2 operation, the *q*-axis current control is active from t=33.543s and makes an effort to maintain the power plant terminal voltage (V_8) at 1p.u. as in Sec. III. However, for *Case* 2 with PFM operation, PFM is active for 1 second after fault duration (from t=33.543s to t=34.543s) and after t=34.543s its action resembles that of *Case* 2 operation. The variation of power plant terminal frequency (f_8) is shown in Fig. 14. The deviation of this frequency from the steady state terminal frequency is taken as input to the PFM operation to modulate the q-axis GSC current command (I^*_{gqref}). This in turn modulates the reactive power exchange of the plant (Q_{dg}) with the grid as shown in Fig. 15. It can be seen that *Case* 2 with PFM modification injects more reactive power during the small post-fault duration in comparison to that of *Case* 2 alone. Injection of reactive power to the grid boosts the terminal voltage (V_8)as can be seen in Fig. 16.

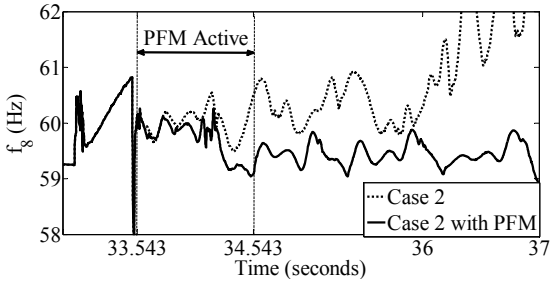

Fig. 14. Variation of wind power plant terminal frequency (f_8) under (i) *Case* 2 and (ii) *Case* 2 with PFM operation

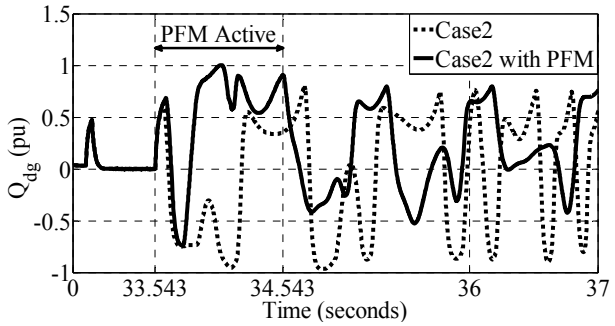

Fig. 15. Variation of wind power plant reactive power injection (Q_{dg}) under (i) *Case* 2 and (ii) *Case* 2 with PFM operation

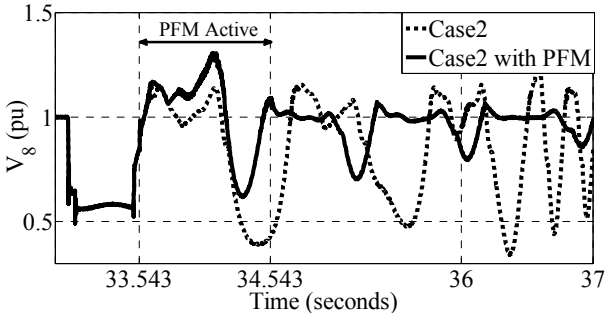

Fig. 16. Variation of wind power plant terminal voltage (V_8) under (i) *Case* 2 and (ii) *Case* 2 with PFM operation

This affects the nearby alternators and hence their terminal voltages rise too. The result is an increase in their power outputs. The variation of alternator 2 output power (P_2) is shown in Fig. 17. It is clear that P_2 is higher for *Case*2 with PFM in comparison to that of *Case* 2 alone during post-fault. An increase in alternator power output means a decrease in the accelerating power of alternators and an improvement in transient stability margin of power systems. This is obvious in Fig. 18 where the relative rotor angle (δ_{21}) is bounded for *Case* 2 with PFM operation whereas it is unbounded for *Case* 2 operation.

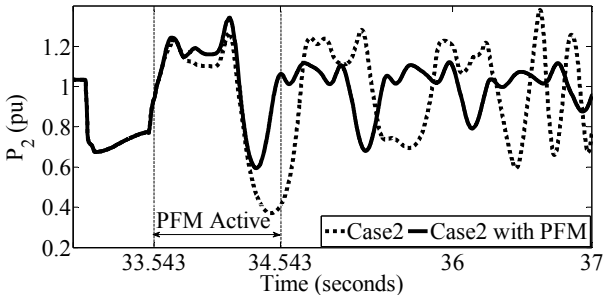

Fig. 17. Variation of alternator 2 output power (P_2) under (i) *Case* 2 and (ii) *Case* 2 with PFM operation

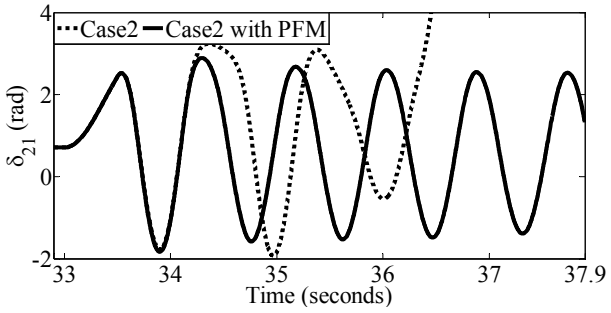

Fig. 18. Variation of relative rotor angle (δ_{21}) under (i) *Case* 2 and (ii) *Case* 2 with PFM operation

CCTs obtained for short circuit faults at bus 4 and bus 5 at different fault instants are presented in Table II. It can be observed that wind power plant if operated under Case 2 with PFM modification increases CCT values at different fault instants and thus improves transient stability of power systems.

TABLE II
Comparison of CCT for *Case* 2 and*Case* 2 with PFM Operation

Fault Bus	Fault Instants	Case 2 (ms)	Case2 with PFM (ms)	Improvement (ms)
Bus 4	X	254	273	**19**
	Y	324	338	**14**
	Z	360	370	**10**
Bus 5	X	333	361	**28**
	Y	492	538	**46**
	Z	576	616	**40**

VI. CONCLUSION

This paper presents two modified control strategies of PMSG based wind power plant to enhance transient stability of power systems. In the first method, the balance grid side converter current is injected as reactive current to the grid at steady state. In the second method, the GSC is controlled to maintain the power plant terminal voltage at a nominal value. Both the methods have been simulated and investigated in WSCC 3-machine 9-bus system in PSCAD/EMTDC platform. The second method is found to be a better choice of the two since it improves transient stability for different fault locations and fault instants. An additional post-fault modification in the GSC control strategy is also proposed in this paper. This post-fault modification when combined with the second method proposed earlier enhances transient stability even more. This is validated in WSCC 3-machine 9-bus system using variable speed profiles in PSCAD/EMTDC software.

ACKNOWLEDGEMENT

The authors would like to thank Department of Science and Technology, New Delhi, India for financially assisting this work through the project numbered, SB/S3/EECE/074/2013.

REFERENCES

[1] Z. Chen, J.M. Guerrero and F. Blaabjerg, "A review of the state of the art of power electronics for wind turbines", *IEEE Trans. Power Electron.* , vol. 24, no. 8, pp. 1859-1875, Aug. 2009.

[2] A. D. Hansen and A. Müfit. "Impact of advanced wind power ancillary services on power system", DTU Wind Energy E, Roskilde, Denmark, no. 0081, 2015.

[3] J.G.Slootweg and W.L.Kling, "Impacts of distributed generation on power system transient stability", in *Proc. IEEE Power Eng. Soc. Sum. Meeting*, vol. 2, *2002*, pp. 862-867.

[4] M.J. Hossain, H.R. Pota, M.A. Mahmud and R.A. Ramos, "Investigation of the impacts of large-scale wind power penetration on the angle and voltage stability of power systems", *IEEE Syst. J*, vol. 6, no. 1, pp 76-84, Mar. 2012.

[5] D. Gautam, V. Vittal and T. Harbour, "Impact of increased penetration of DFIG based wind turbine generators on transient and small signal stability of power systems", *IEEE Trans. Power Syst.*, vol. 24, no.3, pp. 1426-1434, Aug. 2009.

[6] L.Shi, S. Sun, L.Yao, Y. Ni, and M. Bazargan, "Effects of wind generation intermittency and volatility on power system transient stability", *IET Renew. Power Gener.*, vol. 8, no. 2, pp. 717-730, Oct.2014.

[7] M. V. A. Nunes, J. A. P. Lopes, H. H. Zurn, U. H. Bezerra and R. G. Almeida, "Influence of the variable-speed wind generators in transient stability margin of the conventional generators integrated in electrical grids," *IEEE Trans. Energy Convers.*, vol. 19, no. 4, pp. 692-701, Dec. 2004.

[8] J. F. Conroy and R. Watson, "Frequency Response Capability of Full Converter Wind Turbine Generators in Comparison to Conventional Generation", *IEEE Trans. Power Syst.* vol. 23, no. 2, pp. 649-656, May.2008

[9] G. Revel, A. E. Leon, D. M. Alonso and J. L. Moiola, "Dynamics and Stability Analysis of a Power System with a PMSG-Based Wind Farm Performing Ancillary Services" *IEEE Trans. Circuits Syst. I: Reg. Papers*, vol. 61, no. 7, pp. 2182-2193, July.2014.

[10] A. Mitra and D. Chatterjee, "Active Power Control of DFIG-Based Wind Farm for Improvement of Transient Stability of Power Systems", *IEEE Trans. Power Syst.*,vol. 31, no. 1 pp. 82-93, Jan.2016.

[11] J. F. Conroy and R. Watson. "Aggregate modelling of wind farms containing full-converter wind turbine generators with permanent magnet synchronous machines: transient stability studies." *IET Renew. Power Gener.*,vol. 3, no. 1, pp. 39-52, Mar. 2009.

[12] S.M. Muyeen, R. Takahashi, T. Murata and J. Tamura, "A Variable Speed Wind Turbine Control Strategy to Meet Wind Farm Grid Code Requirements", *IEEE Trans. Power Syst.* vol. 25, no. 1, pp. 331-340, Feb. 2010.

[13] H. Geng and D. Xu, "Stability Analysis and Improvements for Variable-Speed Multi-pole Permanent Magnet Synchronous Generator-Based Wind Energy Conversion Systems", *IEEE Trans. Sustain. Energy*, vol. 2, no.4, pp. 459-467, Oct.2011.

[14] S. Huang, Z. Chen, K. Huang and J. Gao, "Maximum torque per ampere and flux-weakening control for PMSM based on curve fitting", in *Proc. IEEE Veh. Power and Propul. Conf. (VPPC),* 2010, pp. 1-5.

[15] A. Yazdani and R. Iravani, Voltage-Sourced Converters in Power Systems, Modeling, Control and Applications, Hoboken, NJ. USA, John Wiley & Sons, 2010.

[16] S. Alepuz, A. Calle, S. Busquets-Monge, S. Kouro and B. Wu, "Use of Stored Energy in PMSG Rotor Inertia for Low-Voltage Ride Through in Back-to-Back NPC Converter-Based Wind Power Systems", *IEEE Trans. Ind. Electron.,* vol. 60, no. 5, pp.1787-1796, May. 2013.

[17] P. Kundur, *Power System Stability and Control*, New York, NY, USA: McGraw-Hill, 1994.

[18] M. K. Donnelly, J.E. Dagle, D.J. Trudnowski and G.J. Rogers, "Impacts of the Distributed Utility on Transmission System Stability", *IEEE Trans. Power Syst.,* vol. 11, no. 2, pp. 741-746, May.1996.

[19] P.W. Sauer and M.A. Pai, *Power System Dynamics and Stability*, Hong Kong: Pearson Education Asia, 2002, First Indian Reprint.

[20] N.G. Hingorani, L. Gyugyi and M. El-Hawary, *Understanding FACTS: concepts and technology of flexible AC transmission systems*. vol. 2. New York: IEEE press, 2000.